

ISSN: 0256-307X

# 中国物理快报

# Chinese Physics Letters

Volume 29 Number 2 February 2012

A Series Journal of the Chinese Physical Society  
Distributed by IOP Publishing

Online: <http://iopscience.iop.org/cpl>  
<http://cpl.iphy.ac.cn>

CHINESE PHYSICAL SOCIETY  
**IOP** Publishing

JUST FOR AUTHORS  
— CHINESE PHYSICS LETTERS

## High Time-Resolved Imaging of Targets in Turbid Media Using Ultrafast Optical Kerr Gate \*

TONG Jun-Yi(佟俊仪), TAN Wen-Jiang(谭文疆), SI Jin-Hai(司金海)\*\*, CHEN Feng(陈烽),  
YI Wen-Hui(易文辉), HOU Xun(侯洵)

Key Laboratory for Physical Electronics and Devices of the Ministry of Education, Shaanxi Key Lab of Information Photonic Technique, School of Electronics and Information Engineering, Xi'an Jiaotong University, Xi'an 710049

(Received 11 November 2011)

*We demonstrate the ultrafast imaging of a submillimeter bar chart that is either hidden behind glass diffusers or inside a solution of polystyrene spheres, using an ultrafast optical Kerr gate (OKG). The results show that the time-resolved imaging of the target in the turbid media with an optical depth of 11.4 is achieved using the OKG with a 1.6 ps opening time. The image contrast is improved by about 70% compared with the shadowgraph imaging.*

PACS: 42.65.-k, 42.62.-b

DOI:10.1088/0256-307X/29/2/024207

Imaging of targets embedded in turbid media are important in industrial, military and biomedical applications. However, it is difficult to observe those targets because of the strong multiple scattering. To overcome this problem, many optical gating techniques have been proposed for optical imaging in turbid media, which include the spatial filtering technique, the coherence-gating technique,<sup>[1]</sup> the time-gating technique<sup>[2-4]</sup> and so on. Compared with spatial filtering, the time-gating technique has the ability to separate the forward scattered diffusive photons traveling collinearly with small diverging angles from ballistic photons with a higher spatial resolution. Compared with the coherence-gating technique, the time-gating technique can use ballistic and near-ballistic light to acquire sufficient signal levels for imaging an object that is hidden in a highly turbid medium.

Imaging of a target in turbid media using the optical Kerr gate (OKG), which is a time gate with mild spatial filtering, could enhance image quality.<sup>[4-7]</sup> Recently, the OKG technique has been adapted for investigating the dynamics of spray breakup and vaporization in the near field of the liquid-fueled combustion of a high-speed rocket spray. The optical depth of the near field is high, while other approaches have failed to reveal the internal structure of this area.<sup>[8-14]</sup> The experimental data from the interior of the injector are important for designing rocket nozzle geometries.

In this Letter, we demonstrate the ultrafast imaging of a target in turbid media using an OKG in the femtosecond time scale, in which the target is hidden either behind glass diffusers or in a solution of polystyrene spheres. The results show that the time-resolved imaging in the turbid media with the optical depth about 11.4 is achieved using the OKG for a 1.6 ps opening time.

When the photons in a laser pulse travel through turbid media, only a few photons keep their coherence and pass through in a straight line without being scattered. These photons are image-bearing ballistic photons and they will exit the turbid media first, because they take the shortest path length. The most randomly scattered photons are called diffusive photons. Slightly scattered photons are referred to as snake photons, which are slightly deviated from the ballistic direction. These photons can be used in imaging when there are insufficient ballistic photons, though with a lower spatial resolution. By selecting the ballistic photons and rejecting the diffusive photons using spatial filtering, time-gated imaging or coherence-based techniques, it is possible to obtain diffraction-limited image resolution. Here the OKG is a time gate, which consists of a pair of calcite-crossed polarizers with a Kerr medium between them. Meanwhile, the spatial dimension of the pump laser pulse radial profile automatically induces a spatial aperture at the Kerr medium. When the ultrafast OKG is opened, only the ballistic and snake photons arriving earlier can pass through the gate. Figure 1 shows schematically the laser pulse passing through turbid media and eliminating the diffusive light from the image-bearing light using OKG.

Imaging through turbid media was performed using an OKG with setup shown in Fig. 2. A Ti:sapphire laser system (FEMTOPOWER compact Pro), emitting 30 fs, 800 nm laser pulses at a repetition rate of 1 kHz, was used in our experiments. The laser beam was split into an imaging beam and a gating beam by using a beam splitter. A delay line was used to control the time delay between the gating pulse and the imaging pulse. The gating beam was focused into the Kerr medium by lens L<sub>1</sub>, and the polarization of the beam was rotated 45° by a  $\lambda/2$  wave plate.

\*Supported by National Basic Research Program of China under Grant No 2012CB921804, and the National Natural Science Foundation of China under Grant Nos 91123028 and 11074197.

\*\*Corresponding author. Email: jinhaisi@mail.xjtu.edu.cn

© 2012 Chinese Physical Society and IOP Publishing Ltd

The linearly polarized imaging beam was introduced into the turbid media. The optical depth is up to 12 (transmission factor of  $\sim 10^{-10}$ ). The disturbed imaging beam emerging from the turbid media was focused into the Kerr medium together with the gating beam. The gating beam overlapped the imaging beam in the Kerr medium to ensure that the ballistic component could pass through the OKG. In addition, very few diffusive photons could be overlapped by the gating beam and pass through the OKG for the limited gating beam radius. The viewing area of the images will increase with the increasing overlapped area between the imaging beam and the gating beam. The OKG consists of a pair of calcite crossed polarizers and a Kerr medium between them. When the gating pulse causes a transient birefringence in the Kerr medium, the imaging beam will pass through the analyzer and be detected by a color charged-coupled device (CCD) camera (NIKON DXM 1200 F).

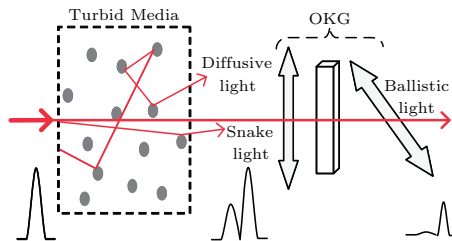


**Fig. 1.** Schematic diagram of a laser pulse passing through turbid media and eliminating the diffusive light from the image-bearing light using the OKG method.

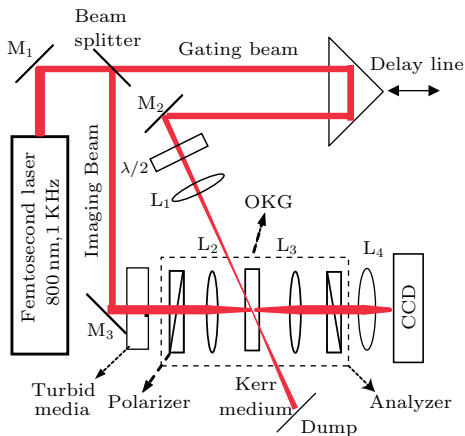


**Fig. 2.** Schematic setup for imaging in turbid media using the OKG method; L: lenses; M: mirrors;  $\lambda/2$ : half wave plate.

In our experiments, the Kerr medium  $\text{CS}_2$  solution was filled in a glass cuvette with a path length of 1 mm. The opening time of the OKG for  $\text{CS}_2$  is estimated to be 1.6 ps. The result is in agreement with the previous reports and indicates the reliability of our experiment.<sup>[15–17]</sup> The measured temporal Kerr intensity profile of the transmitted signal through the solution of polystyrene spheres (0.4  $\mu\text{m}$ ) with the optical depth of 12 is shown in Fig. 3 (hollow circle). We

also plot a reference Kerr signal from the deionized water reference sample (solid square). The ballistic peak corresponds to the incident pulse, and there is no obvious diffusive peak separating from the ballistic peak. The reason is that the diameter of the polystyrene spheres used in our experiment is so small that the forward scattering probability is very low for these particles.<sup>[18]</sup> Therefore, only a few diffusive photons can scatter in the forward direction and pass through the OKG.

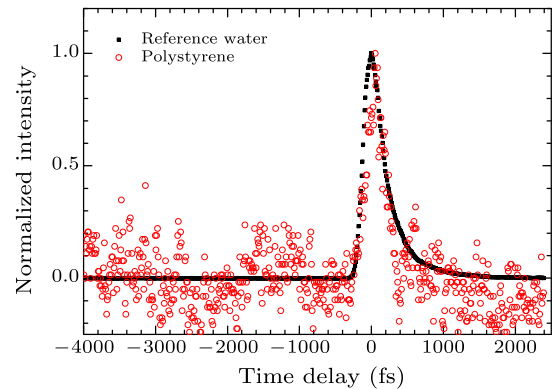


**Fig. 3.** The measured temporal Kerr intensity profile of the transmitted signal through the solution of polystyrene spheres with the optical depth of 12 (hollow circle). We also plot a reference Kerr signal from the deionized water reference sample (solid square).

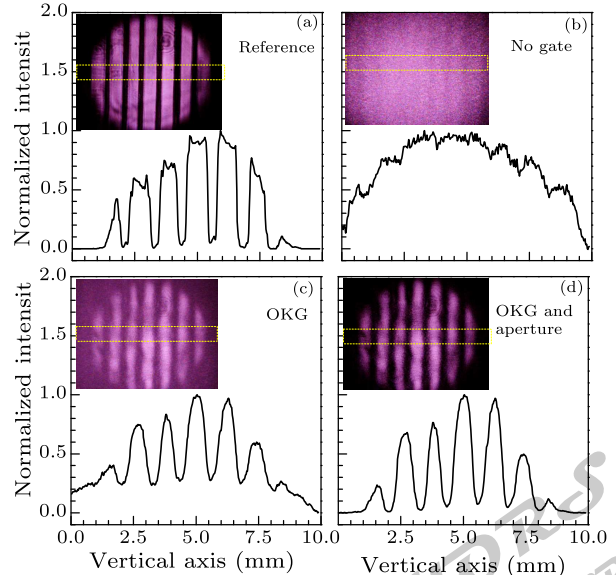


**Fig. 4.** Comparison of diffusive and OKG imaging of a bar chart hidden behind glass diffusers and the corresponding normalized intensity distributions in the rectangle as a function of CCD spatial position. (a) Reference imaging without the glass diffusers (ground glass). (b) Direct shadowgraph imaging. (c) OKG imaging. (d) OKG imaging with an aperture before the CCD.

The target sample is dark bars on a transparency sheet, the width of each bar is about 0.5 mm, and the direct shadowgraph imaging is shown in Fig. 4(a). Figure 4(b) represents the transillumination imaging

of the target bar chart hidden behind the glass diffusers with the optical depth of 7.26, and the image of

the bar chart is blurred. The measurement methods of the optical depth can be consulted in Ref. [19].

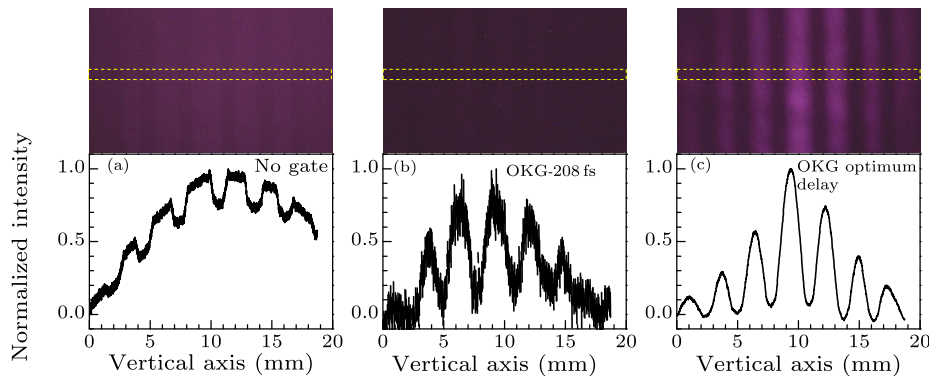


**Fig. 5.** Time-resolved OKG imaging of the target bar chart hidden in the polystyrene spheres of diameter  $0.4\ \mu\text{m}$  suspension and the corresponding normalized intensity distributions in the rectangle as a function of CCD spatial position. (a) Direct shadowgraph imaging. (b) Gating time at  $-208\ \text{fs}$ . (c) Gating time at optimum delay.

To estimate the imaging quality, we calculate the contrast values from the intensity contribution. The contrast of the intensity field is calculated as  $(I_{\text{max}} - I_{\text{min}}) / (I_{\text{max}} + I_{\text{min}})$ , where  $I_{\text{max}}$  and  $I_{\text{min}}$  are the maximum and minimum image intensities, respectively. Assuming that the value of the contrast of the image in Fig. 4(a) is 1, and the value in Fig. 4(b) by direct shadowgraph imaging decreases to about 3%. Figure 4(c) presents the image using the OKG imaging technique, in which most of the diffusive photons are separated from the ballistic photons. The image contrast is increased to about 38% compared to the shadowgraph imaging, but there are some noises coming from the scattering pump pulse. Because the output laser beam has a Gaussian intensity profile, the normalized intensity of the image is stronger in the center than at the edges. The gating beam background signal noise also has a Gaussian intensity profile, as shown in Fig. 4(c), which causes the contrasts of the image to be non-unique for the center and the edges. To reduce these noises, in the experiment an aperture was added before the CCD and the estimated contrast increased to about 76% in comparison to the shadowgraph image shown in Fig. 4(d).

As an alternative turbid medium, a water solution of polystyrene spheres with diameter of  $0.4\ \mu\text{m}$  was used. The solution was filled in a quartz cell with thickness of 10 mm and the target bar chart was embedded in the middle of the cell and the optical depth measured to be about 11.4. Figure 5(a) shows the direct shadowgraph imaging of the target bars hidden in the polystyrene sphere suspension and the image was blurred. Figures 5(b) and 5(c) show the images of the target bar using the OKG at the non-optimum delay and the optimum delay between the image and the pump pulse. When the gating pulse arrived 208 fs

earlier than the optimum delay, the bar chart is hard to see and the image contrast is poor, as shown in Fig. 5(b). Figure 5(c) shows the clear bar chart image at the optimum delay between the imaging and the gating pulse and the contrast is improved from about 16% to 87%. The results suggest the feasibility of the imaging of targets hidden in turbid media using the OKG technique with submillimeter spatial resolution.

In summary, we have demonstrated the ultrafast imaging of a target in turbid media using an OKG for a 1.6 ps opening time. The results show that the time-resolved imaging of the submillimeter bar chart in the turbid media with optical depth of about 11.4 are achieved using the OKG and the image contrasts using the OKG are improved by about 70% in comparison with using direct shadowgraph imaging.

## References

- [1] Huang D et al 1991 *Science* **254** 1178
- [2] Yoo K M and Alfano R R 1990 *Opt. Lett.* **15** 320
- [3] Fujimoto J G et al 1986 *Opt. Lett.* **11** 150
- [4] Wang L et al 1991 *Science* **253** 769
- [5] Alfano R R et al 1994 *Science* **264** 1913
- [6] Wang L et al 1993 *Opt. Lett.* **18** 241
- [7] Wang L, Ho P P and Alfano R R 1993 *Appl. Opt.* **32** 535
- [8] Paciaroni M and Linne M 2004 *Appl. Opt.* **43** 5100
- [9] Paciaroni M et al 2006 *Atomization and Sprays* **16** 51
- [10] Gord J et al 2005 *Appl. Opt.* **44** 6627
- [11] Hall T et al 2006 *Exp. Fluids* **40** 836
- [12] Sedarsky D L et al 2006 *Opt. Lett.* **31** 906
- [13] Schmidt J B et al 2008 *Appl. Opt.* **48** B137
- [14] Idlahcen S, Blaisot J B, Girasole T Rozé and Mées L 2008 *14th International Symposium on Applications of Laser Techniques to Fluid Mechanics* (Lisbon, Portugal, 7–10 July 2008)
- [15] Yan L et al 2009 *IEEE Photon. Technol. Lett.* **21** 1606
- [16] Tan W et al 2010 *J. Appl. Phys.* **107** 043104
- [17] Kalpouzos C et al 1987 *J. Phys. Chem.* **91** 2028
- [18] Berrócal E et al 2007 *Opt. Express* **15** 10649
- [19] Tong J et al 2011 *Opt. Eng.* **50** 043607

# Chinese Physics Letters

Volume 29

Number 2

February 2012

## GENERAL

- 020201 **Mei Symmetry and New Conserved Quantities of Tzénoff Equations for the Variable Mass Higher-Order Nonholonomic System**  
ZHENG Shi-Wang, WANG Jian-Bo, CHEN Xiang-Wei, XIE Jia-Fang
- 020202 **Generation of a New Coupled Ultra-Short Pulse System from a Group Theoretical Viewpoint: the Cartan Ehresman Connection**  
Saliou Youssoufa, Victor K. Kuetche, Timoleon C. Kofane
- 020203 **Periodic Wave Solutions to a (3+1)-Dimensional Soliton Equation**  
WANG Jun-Min
- 020301 **The Anisotropy of Dipolar Condensate in One-Dimensional Optical Lattices**  
TIE Lu, XUE Ju-Kui
- 020302 **Decoherence and Multipartite Entanglement of Non-Inertial Observers**  
M. Ramzan
- 020303 **Approximate Analytical Solutions to the Generalized Pöschl–Teller Potential in  $D$  Dimensions**  
Hassanabadi Hassan, Yazarloo Bentol Hoda, LU Liang-Liang
- 020401 **Entropy Conservation in the Transition of Schwarzschild-de Sitter Space to de Sitter Space through Tunneling**  
ZHANG Bao-Cheng, CAI Qing-Yu, ZHAN Ming-Sheng
- 020501 **Generating a New Higher-Dimensional Ultra-Short Pulse System: Lie-Algebra Valued Connection and Hidden Structural Symmetries**  
Hermann T. Tchokouansi, Victor K. Kuetche, Abbagari Souleymanou, Thomas B. Bouetou, Timoleon C. Kofane
- 020502 **Adaptive Generalized Projective Synchronization of Takagi-Sugeno Fuzzy Drive-response Dynamical Networks with Time Delay**  
ZHENG Yong-Ai
- 020503 **Adaptive Third-Order Leader-Following Consensus of Nonlinear Multi-agent Systems with Perturbations**  
SUN Mei, CHEN Ying, CAO Long, WANG Xiao-Fang
- 020504 **Mechanisms for Oscillations in Volume of Single Spherical Bubble Due to Sound Excitation in Water**  
REN Sheng, ZHANG Jia-Zhong, LI Kai-Lun
- 020505 **Generalized Projective Synchronization of Fractional Order Chaotic Systems with Different Dimensions**  
WANG Sha, YU Yong-Guang
- 020701 **Fabrication and Performance of Micro-sensors for Methane Detection Based on In-Pd-Co-SnO<sub>2</sub> Composite Nanofibers**  
QIAO Ji-Ping, ZHU Zi-Peng, YAN Xiao-Yan, QIN Jian-Min

## THE PHYSICS OF ELEMENTARY PARTICLES AND FIELDS

- 021101 **Analysis of the Vertexes  $\Sigma_Q \Xi_Q^* K^*$  and  $\Xi'_Q \Sigma_Q^* K^*$  within Light-Cone QCD Sum Rules**  
YOU Fu-Yi, WANG Zhi-Gang, WAN Shao-Long
- 021102 **Electron-Positron Pair Production in an Elliptic Polarized Time Varying Field**  
XIE Bai-Song, Mohamedsedik Melike, Dulat Sayipjamal

## NUCLEAR PHYSICS

- 022101 **Analyses of  $\beta$ -Bands of  $^{230,232}\text{Th}$  and  $^{232,234}\text{U}$  by the Projected Shell Model**  
CUI Ji-Wei, ZHOU Xian-Rong, CHEN Fang-Qi, SUN Yang, WU Cheng-Li

- 022102 Identification of a New Four-Quasiparticle State in Odd-Odd  $^{186}\text{Au}$**   
 LI Shi-Cheng, SHI Yue, ZHANG Yu-Hu, ZHOU Xiao-Hong, XU Fu-Rong, FANG Yong-De,  
 LIU Min-Liang, DING Bing, GUO Song, LI Guang-Shun, ZHOU Hou-Bing, M. Oshima, Y. Toh, M.  
 Koizumi, A. Osa, A. Kimura, Y. Hatsukawa, H. Hayakawa, T. Shizuma, J. Katakura, M. Matsuda, T.  
 Morikawa, M. Sugawara, H. Kusakari
- 022501 Ansatz, Assumptions and Production of  $J/\Psi$ -Particles: A Non-charmed Approach versus Charmed Ones**  
 P. Guptaroy, Goutam Sau, S. Bhattacharyya
- 022502 Energy and Centrality Dependences of Pseudorapidity Distributions of Charged Particles in Cu+Cu Collisions**  
 JIANG Zhi-Jin, SUN Yu-Fen

#### ATOMIC AND MOLECULAR PHYSICS

- 023201 Temperature Dependence of Atomic Decay Rate**  
 ZHANG Jian-Jun, CHENG Ze
- 023701 Measurement of Spatial Distribution of Cold Atoms in an Integrating Sphere**  
 WANG Xu-Cheng, CHENG Hua-Dong, XIAO Ling, ZHENG Ben-Chang, MENG Yan-Ling, LIU Liang,  
 WANG Yu-Zhu

#### FUNDAMENTAL AREAS OF PHENOMENOLOGY(INCLUDING APPLICATIONS)

- 024201 Ultrashort Pulse Generation at Quasi-40-GHz by Using a Two-Section Passively Mode-Locked InGaAsP-InP Tensile Strained Quantum-Well Laser**  
 KONG Duan-Hua, ZHU Hong-Liang, LIANG Song, QIU Ji-Fang, ZHAO Ling-Juan
- 024202 Two-Photon Atomic Coherence Effect of Transition  $5S_{1/2}-5P_{3/2}-4D_{5/2}(4D_{3/2})$  of  $^{85}\text{Rb}$  atoms**  
 DING Dong-Sheng, ZHOU Zhi-Yuan, SHI Bao-Sen, ZOU Xu-Bo, GUO Guang-Can
- 024203 Three-Dimensional Thermal Analysis of 18-Core Photonic Crystal Fiber Lasers**  
 ZHENG Yi-Bo, YAO Jian-Quan, ZHANG Lei, WANG Yuan, WEN Wu-Qi, JING Lei, DI Zhi-Gang
- 024204 A Dual-Crystal Cavity Ho,Tm:GdVO<sub>4</sub> Laser**  
 ZHU Guo-Li, JU You-Lun, YAO Bao-Quan, WANG Yue-Zhu
- 024205 Realization of a Two-Dimensional Magneto-optical Trap with a High Optical Depth**  
 LIU Yang, WU Jing-Hui, SHI Bao-Sen, GUO Guang-Can
- 024206 A 200 kHz Q-Switched Adhesive-Free Bond Composite Nd:YVO<sub>4</sub> Laser using a Double-Crystal RTP Electro-optic Modulator**  
 YU Yong-Ji, CHEN Xin-Yu, WANG Chao, WU Chun-Ting, LIU Rui, JIN Guang-Yong
- 024207 High Time-Resolved Imaging of Targets in Turbid Media Using Ultrafast Optical Kerr Gate**  
 TONG Jun-Yi, TAN Wen-Jiang, SI Jin-Hai, CHEN Feng, YI Wen-Hui, HOU Xun
- 024208 A New Method for Electromagnetic Time Reversal in a Complex Environment**  
 KONG Qi, SHI Qing-Fan, YU Guang-Ze, ZHANG Mei
- 024209 Escaped and Trapped Emission of Organic Light-Emitting Diodes**  
 LIANG Shi-Xiong, WU Zhao-Xin, ZHAO Xuan-Ke, HOU Xun
- 024210 Influence of Microwave Detuning on Ramsey Fringes of a Single Nitrogen Vacancy Center Spin in Diamond**  
 HU Xin, LIU Gang-Qin, XU Zhang-Cheng, PAN Xin-Yu
- 024301 Further Notes on the Gaussian Beam Expansion**  
 DAI Yu-Rong, DING De-Sheng
- 024302 Surface Acoustic Wave Propagation in Relaxor-Based Ferroelectric Single Crystals  $0.93\text{Pb}(\text{Zn}_{1/3}\text{Nb}_{2/3})\text{O}_3-0.07\text{PbTiO}_3$  Poled along  $[011]_c$**   
 LI Xiu-Ming, ZHANG Rui, HUANG Nai-Xing, LÜ Tian-Quan, CAO Wen-Wu
- 024701 Finite Spectral Semi-Lagrangian Method for Incompressible Flows**  
 LI Shao-Wu, WANG Jian-Ping

- 024702 **Axisymmetric Stagnation-Point Flow with a General Slip Boundary Condition over a Lubricated Surface**  
M. Sajid, K. Mahmood, Z. Abbas
- 024703 **A Lattice Boltzmann Method for Simulating the Separation of Red Blood Cells at Microvascular Bifurcations**  
SHEN Zai-Yi, HE Ying

#### PHYSICS OF GASES, PLASMAS, AND ELECTRIC DISCHARGES

- 025201 **The Key Factor for Uniform and Patterned Glow Dielectric Barrier Discharge**  
OUYANG Ji-Ting, DUAN Xiao-Xi, XU Shao-Wei, HE Feng
- 025202 **Transport Properties of Lithium Plasma**  
CHEN Shi-Qiang, WANG Hai-Xing
- 025203 **Excitation of Internal Kink Mode by Circulating Supra-thermal Electrons**  
CHEN Shao-Yong, WANG Zhong-Tian, TANG Chang-Jian
- 025204 **Comparison of Dust Lattice Waves in Three-Dimensional Cubic Configurations**  
B. Farokhi, A. Hameditabar

#### CONDENSED MATTER: STRUCTURE, MECHANICAL AND THERMAL PROPERTIES

- 026101 **Dislocation and Elastic Strain in an InN Film Characterized by Synchrotron Radiation X-Ray Diffraction and Rutherford Backscattering/Channeling**  
CHENG Feng-Feng, FA Tao, WANG Xin-Qiang, YAO Shu-De
- 026102 **High-Pressure and High-Temperature *in situ* X-Ray Diffraction Study of FeP<sub>2</sub> up to 70 GPa**  
GU Ting-Ting, WU Xiang, QIN Shan, LIU Jing, LI Yan-Chun, ZHANG Yu-Feng
- 026103 **Microscopic Phase-Field Study of the Occupancy Probability of  $\alpha$  Sublattices Involving Coordination Environmental Difference for D<sub>022</sub>-Ni<sub>3</sub>V**  
ZHANG Jing, CHEN Zheng, ZHUANG Hou-Chuan, LU Yan-Li
- 026201 **Deformation Induced Internal Friction Peaks in Nanocrystalline Nickel**  
LI Ping-Yun, ZHANG Xi-Yan, NI Hai-Tao, CAO Zhen-Hua, MENG Xiang-Kang
- 026501 **A Temperature Sensor Based on a Symmetrical Metal-Cladding Optical Waveguide**  
ZHOU Guo-Rui, FENG Guo-Ying, ZHANG Yi, MA Zi, WANG Jian-Jun
- 026801 **Morphological Evolution of a-GaN on r-Sapphire by Metalorganic Chemical Vapor Deposition**  
SANG Ling, LIU Jian-Ming, XU Xiao-Qing, WANG Jun, ZHAO Gui-Juan, LIU Chang-Bo, GU Cheng-Yan, LIU Gui-Peng, WEI Hong-Yuan, LIU Xiang-Lin, YANG Shao-Yan, ZHU Qin-Sheng, WANG Zhan-Guo
- 026802 **Wetting Behavior between Droplets and Dust**  
YU Yang, WU Qun, WANG Xue-Wei, YANG Xiao-Bin

#### CONDENSED MATTER: ELECTRONIC STRUCTURE, ELECTRICAL, MAGNETIC, AND OPTICAL PROPERTIES

- 027101 **Resonant Tunneling States of a Pairing Ladder with Random Dimer Chains**  
HU Dong-Sheng, ZHANG Yan-Ling, YIN Xiao-Gang, ZHU Chen-Ping, ZHANG Yong-Mei
- 027102 **Voltage-Induced Effect on Resistance of C:N/Si Heterojunctions**  
GAO Xi-Li, ZHANG Xiao-Zhong, WAN Cai-Hua, WANG Ji-Min
- 027301 **Effect of Thin Metallic Layers on the Refractive Index of a Multilayer System**  
A. Ozturk, R. Suleymanli, B. Aktas, A. Teber
- 027302 **Alternating-Current Transport Properties of the Interface between Nd<sub>0.7</sub>Sr<sub>0.3</sub>MnO<sub>3</sub> Ceramic and a Ag Electrode**  
CHEN Shun-Sheng, YANG Chang-Ping, LUO Xiao-Jing, Bärner K., Medvedeva I. V.
- 027303 **Improving Breakdown Behavior by Substrate Bias in a Novel Double Epi-layer Lateral Double Diffused MOS Transistor**  
LI Qi, WANG Wei-Dong, LIU Yun, WEI Xue-Ming

- 027501 Domain Rotation Simulation of the Magnetostriction Jump Effect of  $\langle 110 \rangle$  Oriented TbDyFe Crystals**  
ZHANG Chang-Sheng, MA Tian-Yu, PAN Xing-Wen, YAN Mi
- 027502 Adiabatic Magneto-optical and Magnetocaloric Effects of  $\text{Tb}_3\text{Ga}_5\text{O}_{12}$  at Low Temperature in Strong Magnetic Fields**  
ZHANG Guo-Ying, CHEN Hui, YANG Dan, HU Feng, LIU Hai-Shun
- 027701 High-Temperature Permittivity and Data-Mining of Silicon Dioxide at GHz Band**  
YUAN Jie, WEN Bo, HOU Zhi-Ling, LU Ming-Ming, CAO Wen-Qiang, BA Chuan, FANG Xiao-Yong, CAO Mao-Sheng
- 027801 Effect of N-Doping on Absorption and Luminescence of Anatase  $\text{TiO}_2$  Films**  
XIANG Xia, SHI Xiao-Yan, GAO Xiao-Lin, JI Fang, WANG Ya-Jun, LIU Chun-Ming, ZU Xiao-Tao
- 027802 Thermoluminescence Responses of Photon and Electron Irradiated Ge- and Al-Doped  $\text{SiO}_2$  Optical Fibres**  
H. Wagiran, I. Hossain, D. Bradley, A. N. H. Yaakob, T. Ramli
- 027803 Raman Scattering Study of  $\text{In}_x\text{Ga}_{1-x}\text{N}$  Alloys with Low Indium Compositions**  
TENG Long, ZHANG Rong, XIE Zi-Li, TAO Tao, ZHANG Zhao, LI Ye-Cao, LIU Bin, CHEN Peng, HAN Ping, ZHENG You-Dou
- 027804 Guided Mode Resonance Transmission Filters Working at the Intersection Region of the First and Second Leaky Modes**  
MA Jian-Yong, FAN Yong-Tao
- 027805 Abnormal Dielectric Response in an Optical Range Based on Electronic Transition in Rare-Earth-Ion-Doped Crystals**  
FU Xiao-Jian, XU Yuan-Da, ZHOU Ji

**CROSS-DISCIPLINARY PHYSICS AND RELATED AREAS OF SCIENCE AND TECHNOLOGY**

- 028501 AlGaIn/GaN Metal-Insulator-Semiconductor High Electron-Mobility Transistor Using a  $\text{NbAlO}/\text{Al}_2\text{O}_3$  Laminated Dielectric by Atomic Layer Deposition**  
BI Zhi-Wei, HAO Yue, FENG Qian, GAO Zhi-Yuan, ZHANG Jin-Cheng, MAO Wei, ZHANG Kai, MA Xiao-Hua, LIU Hong-Xia, YANG Lin-An, MEI Nan, CHANG Yong-Ming
- 028502 Reconfigurable Threshold Logic Element with SET and MOS Transistors**  
WEI Rong-Shan, CHEN Jin-Feng, CHEN Shou-Chang, HE Ming-Hua
- 028901 Principle Fluctuation Modes of the Global Stock Market**  
YAN Yan, LIU Mao-Xin, ZHU Xiao-Wu, CHEN Xiao-Song
- 028902 Epidemic Spreading in a Multi-compartment System**  
GAO Zong-Mao, GU Jiao, LI Wei

JUST FOR AUTHORS  
— CHINESE PHYSICS LETTERS